the fitness of sires and sons. Natural selection favors large size in adult males (*17*), and dams produce more sons via large sires [Fig. 1 and (*8*)]. Body size is heritable from sire to son (*18*), and selection on juvenile viability favors large size and early hatch date in male progeny (Fig. 2). Consequently, large sires have high adult fitness and produce sons with high juvenile fitness (Fig. 3). Given the heritability of adult body size (*18*), large sires presumably also produce sons with high adult fitness. This differs from systems in which fitness is not heritable within males (*9*, *11*) because of the accumulation of sexually antagonistic genes on the X chromosome (*10*, *22*, *23*), which does not pass from sire to son. The mechanism of sex determination is unknown in brown anoles, but related *Anolis* species exhibit XY and XXY male heterogamety or genetic sex determination without heteromorphic sex chromosomes (*24*, *25*).

Second, in other species, males with high fitness often sire daughters with low fitness (*8*–*13*). This negative intersexual heritability of fitness may be common when sexually antagonistic X-linked genes are inherited from sire to daughter (*8*, *10*). However, the outcome of good-genes mate choice is complex and likely varies with patterns of sex linkage (*26*). Moreover, intersexual genetic correlations are often reduced or negative for sexually dimorphic traits (*27*–*29*), and the intersexual genetic correlation for body size is actually negative in brown anoles (*18*). This suggests that potential sexual conflict over body size has been largely resolved. Indeed, we found no evidence that large sires produce low-fitness daughters (Fig. 3). In this situation, any potential genetic benefits of mate choice should be preserved, contrary to the situation when high-fitness sires produce low-fitness daughters (*9*–*11*).

Our study suggests that indirect genetic benefits can be obtained even in the face of intralocus sexual conflict. However, this outcome is likely contingent on the evolution of mechanisms that resolve sexual conflict, thereby facilitating sex-specific inheritance and expression of good genes. In brown anoles, these mechanisms may include cryptic sex-ratio bias, which would allow females to preferentially produce high-fitness sons, and negative intersexual genetic correlations, which would mitigate the potential costs of producing low-fitness daughters. Because the underlying physiological mechanisms that produce cryptic sex-ratio bias are presently unknown, we cannot reject the alternative that this bias reflects differential embryonic mortality of sons and daughters with respect to sire size. Given the emerging perspective that intralocus sexual conflict can maintain genetic variation and constrain evolution via mate choice (*8*–*10*), further investigation of these mechanisms should clarify the implications of sexual conflict for a variety of fundamental evolutionary processes.

References and Notes

1. R. M. Cox, R. Calsbeek, *Am. Nat.* **173**, 176 (2009).
2. R. Lande, *Evolution* **34**, 292 (1980).
3. L. F. Delph, J. L. Gehring, F. M. Frey, A. M. Arntz, M. Levri, *Evolution* **58**, 1936 (2004).
4. D. J. Fairbairn, D. A. Roff, *Heredity* **97**, 319 (2006).
5. S. Bedhomme, A. K. Chippindale, in *Sex, Size and Gender Roles: Evolutionary Studies of Sexual Size Dimorphism*, D. J. Fairbairn, W. U. Blanckenhorn, T. Szekely, Eds. (Oxford Univ. Press, Oxford, 2007), pp. 185–194.
6. T. Chapman, G. Arnqvist, J. Bangham, L. Rowe, *Trends Ecol. Evol.* **18**, 41 (2003).
7. G. Arnqvist, L. Rowe, *Sexual Conflict* (Monographs in Behavior and Ecology, Princeton Univ. Press, Princeton, NJ, 2000).
8. K. Foerster *et al*., *Nature* **447**, 1107 (2007).
9. A. Pischedda, A. K. Chippindale, *PLoS Biol.* **4**, e356 (2006).
10. T. Connallon, E. Jakubowski, *Evolution* **63**, 2179 (2009).
11. K. M. Fedorka, T. A. Mousseau, *Nature* **429**, 65 (2004).
12. A. K. Chippindale, J. R. Gibson, W. R. Rice, *Proc. Natl. Acad. Sci. U.S.A.* **98**, 1671 (2001).
13. R. Calsbeek, B. Sinervo, *J. Evol. Biol.* **17**, 464 (2004).
14. W. R. Rice, A. K. Chippindale, *J. Evol. Biol.* **14**, 865 (2001).
15. S. R. Pryke, S. C. Griffith, *Science* **323**, 1605 (2009).
16. R. M. Cox, D. S. Stenquist, R. Calsbeek, *J. Evol. Biol.* **22**, 1586 (2009).
17. R. M. Cox, R. Calsbeek, *Evolution* **64**, 798 (2010).
18. R. Calsbeek, C. Bonneaud, *Evolution* **62**, 1137 (2008).
19. Materials and methods are available as supporting material on *Science* Online.
20. R. R. Tokarz, *Herpetologica* **54**, 388 (1998).
21. R. L. Trivers, *Evolution* **30**, 253 (1976).
22. W. F. Rice, *Evolution* **38**, 735 (1984).
23. J. R. Gibson, A. K. Chippindale, W. R. Rice, *Proc. Biol. Sci.* **269**, 499 (2002).
24. G. C. Gorman, L. Atkins, *Am. Nat.* **100**, 579 (1966).
25. F. J. Janzen, P. C. Phillips, *J. Evol. Biol.* **19**, 1775 (2006).
26. M. Kirkpatrick, D. W. Hall, *Evolution* **58**, 683 (2004).
27. R. Bonduriansky, L. Rowe, *Evolution* **59**, 1965 (2005).
28. E. I. Svensson, A. G. McAdam, B. Sinervo, *Evolution* **63**, 3124 (2009).
29. J. Poissant, A. J. Wilson, D. W. Coltman, *Evolution* **64**, 97 (2010).

30. We thank M. C. Duryea and M. Najarro for genotyping samples and conducting paternity analyses and M. Callahan, D. Cheney, and L. Symes for assistance with mating trails and animal care. M. C. Duryea, S. Kuchta, M. Logan, M. Najarro, and D. Urbach provided comments on the manuscript. Research was conducted under permits from the Bahamas Ministry of Agriculture and approval from the Dartmouth College Institutional Animal Care and Use Committee (protocol 07-02-03). An award from NSF (DEB 0816862 to R. Calsbeek) and funding from Dartmouth College provided financial support.

Supporting Online Material

www.sciencemag.org/cgi/content/full/science.1185550/DC1
Materials and Methods
Fig. S1
References

4 December 2009; accepted 23 February 2010
Published online 4 March 2010;
10.1126/science.1185550
Include this information when citing this paper.

Partitioning of Histone H3-H4 Tetramers During DNA Replication–Dependent Chromatin Assembly

Mo Xu,[1,2]* Chengzu Long,[2]* Xiuzhen Chen,[3,2] Chang Huang,[4,2] She Chen,[2]† Bing Zhu[2]†

Semiconservative DNA replication ensures the faithful duplication of genetic information during cell divisions. However, how epigenetic information carried by histone modifications propagates through mitotic divisions remains elusive. To address this question, the DNA replication–dependent nucleosome partition pattern must be clarified. Here, we report significant amounts of H3.3-H4 tetramers split in vivo, whereas most H3.1-H4 tetramers remained intact. Inhibiting DNA replication–dependent deposition greatly reduced the level of splitting events, which suggests that (i) the replication-independent H3.3 deposition pathway proceeds largely by cooperatively incorporating two new H3.3-H4 dimers and (ii) the majority of splitting events occurred during replication-dependent deposition. Our results support the idea that "silent" histone modifications within large heterochromatic regions are maintained by copying modifications from neighboring preexisting histones without the need for H3-H4 splitting events.

Histone and DNA modifications provide key epigenetic information (*1*–*3*). A newly synthesized DNA strand acquires its DNA methylation pattern by copying the preexisting DNA methylation signature from the template strand (*1*, *4*, *5*). However, the mechanism by which patterns of histone modifications are passed on to daughter cells through mitotic divisions remains enigmatic. To understand this, the DNA replication–dependent nucleosome partition pattern must be unveiled first. Initial studies indicated that the nucleosomes do not dissociate (*6*, *7*), which was amended by the discoveries of "hybrid nucleosomes" that contain old H3-H4 tetramers and new H2A-H2B dimers or vice versa (*8*–*11*). Nevertheless, H3-H4 tetramers—the core particles of nucleosomes—do not dissociate during replication-dependent nucleosome assembly (*12*–*15*). Because all six major lysine methylation sites are present on either H3 (Lys4/9/27/36/79) or H4 (Lys20), newly deposited nucleosomes may become methyl-

[1]Graduate Program, Peking Union Medical College and Chinese Academy of Medical Sciences, Beijing 100730, People's Republic of China. [2]National Institute of Biological Sciences, 7 Science Park Road, Zhong Guan Cun Life Science Park, Beijing 102206, People's Republic of China. [3]Life Science College, Beijing Normal University, Beijing 100875, People's Republic of China. [4]Department of Biochemistry, College of Biological Sciences, China Agricultural University, Beijing 100094, People's Republic of China.

*These authors contributed equally to this work.
†To whom correspondence should be addressed. E-mail: zhubing@nibs.ac.cn (B.Z.); chenshe@nibs.ac.cn (S.C.)

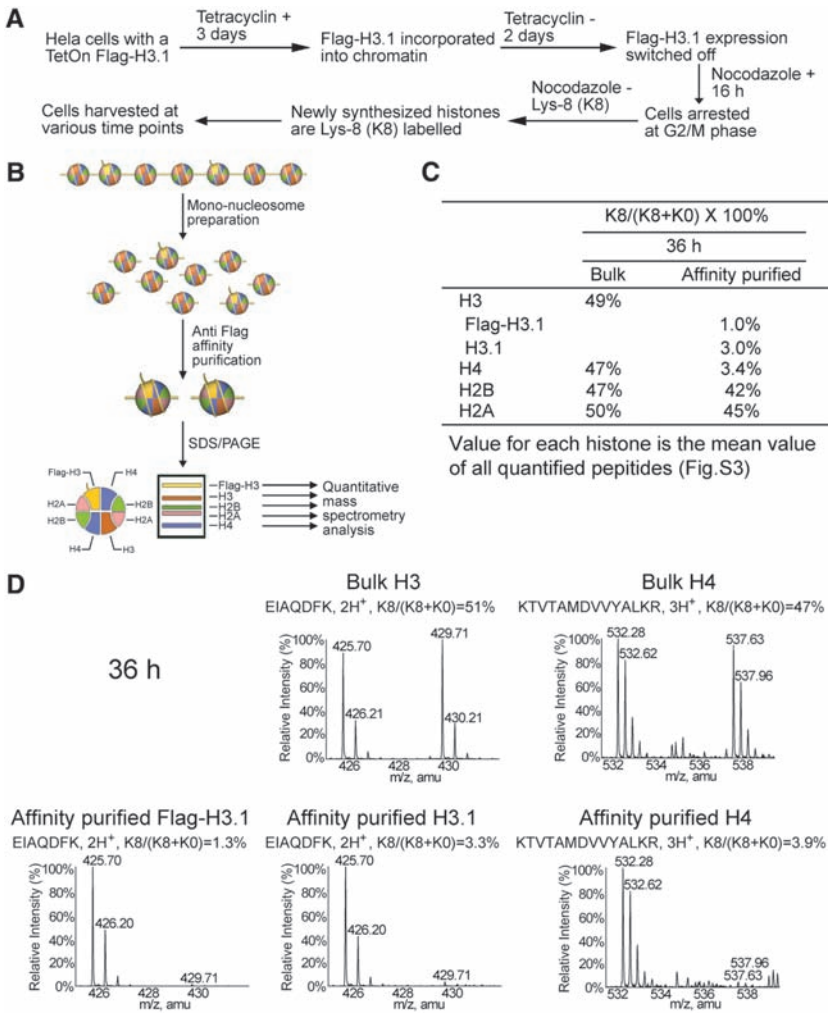

Fig. 1. H3.1-H4 tetramers do not split. (**A** and **B**) Experimental schemes. (**C**) Summary of K8-labeling status of bulk and affinity-purified histones. (**D**) Representative mass spectra for peptides derived from bulk H3, H4, and affinity-purified Flag-H3.1, H3.1, and H4.

A

	K8/(K8+K0) X 100%			
	36 h		72 h	
	Bulk	Affinity purified	Bulk	Affinity purified
H3	37%		76%	
Flag-H3.3		0.3%		2.8%
H3.3		6.4%		23%
H4	36%	3.3%	79%	7.4%
H2B	36%	40%	75%	77%
H2A	40%	40%	83%	72%

Value for each histone is the mean value of all quantified pepitides (Fig.S5)

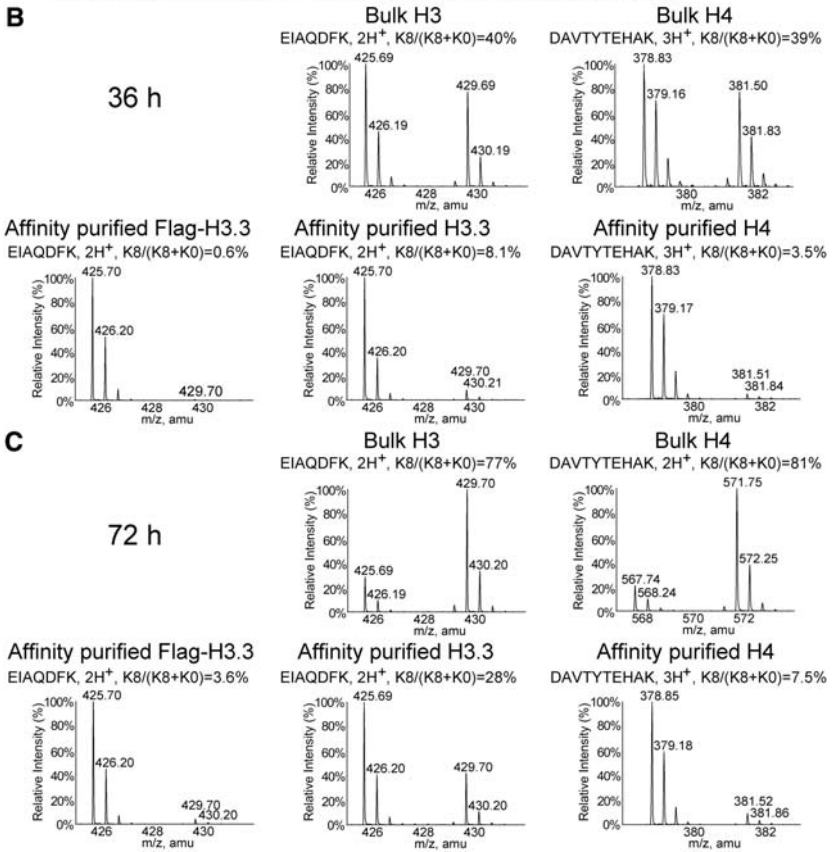

Fig. 2. Significant amounts of H3.3-H4 tetramers split. (**A**) Summary of K8-labeling status of bulk and affinity-purified histones. (**B** and **C**) Representative mass spectra for peptides derived from bulk H3, H4, affinity-purified Flag-H3.3, H3.3, and H4.

ated by "copying" the modification pattern from nearby parental nucleosomes (*1*). However, evidence that the H3-H4 tetramers may split emerged with the discoveries that H3-H4 histones deposit into chromatin as dimers rather than as tetramers (*16*–*18*) and that the histone chaperone Asf1 is capable of disrupting H3-H4 tetramers to form H3-H4/Asf1 heterotrimers (*19*). Thus, the H3-H4 tetramer partitioning pattern needs a definitive reexamination (*1*). In addition, H3.3 variant histones do not form hybrid nucleosomes with canonical H3 histones in vivo (*16*), and they differ from canonical H3 histones for their chromatin localization, chaperon choice, deposition timing, posttranslational modifications, and functions (*16*, *20*–*22*), thus the partitioning pattern of H3.3–containing tetramers is also highly interesting.

We first established stable HeLa cell lines with N-terminally Flag-tagged histone H3.1 or H3.3 under the control of a tetracycline-inducible promoter. To differentiate the "new" histones from the "old" ones and to calculate their ratio, lysine-8 ([$^{13}C_6$, $^{15}N_2$] heavy isotope–labeled L-lysine, abbreviated as K8 for its 8-dalton mass increase from normal lysine) was used in combination with a cell-cycle arrest reagent (nocodazole), thus specifically labeling the "newly synthesized" histones with K8 while leaving the old histones unlabeled (Fig. 1A). By timing the induction with tetracycline, Flag-H3 histones could be designated as old histones or new ones. In addition, we could also study the two major H3 variants, H3.1 and H3.3, individually. Mononucleosomes were prepared from cells with Flag-H3 incorporated into their chromatin (Fig. 1B and fig. S1C) and subjected to affinity purification with antibody to Flag, which selectively purified Flag-H3–containing mononucleosomes (Fig. 1B and fig. S1D). Flag-H3 histones were associated with native H3 and other core histones, as expected (fig. S1D). Flag-H3, copurified native H3, and other core histones were effectively separated by using 13% SDS–polyacrylamide gel electrophoresis (SDS-PAGE) (fig. S1D). Each histone band was excised individually and subjected to SILAC [stable isotope labeling with amino acids in cell culture (*23*)]–based quantitative mass spectrometry analysis. The percentage of new (K8) and old (K0) histones in each band was subsequently calculated (see the explanatory illustration in fig. S2).

At 36 hours after cell-cycle release, all cells had gone through the first S phase, with a vast majority of the cells at either the first G_2/M phase or the second G_1 phase; at 72 hours, all cells had gone through two complete cell cycles, with some cells advancing through the third S phase. These observations were supported by the percentage of K8-labeled bulk histones (Fig. 1 and fig. S3) and with flow cytometry analysis (fig. S3).

After 36 hours of K8 labeling, bulk core histones were approximately half light (K0) and half heavy (K8) (Fig. 1, C and D, and fig. S3), which corresponds to one round of histone deposition. Affinity-purified Flag-H3.1 histones were only 1.0% K8 labeled (Fig. 1, C and D, and fig. S3), demonstrating that they indeed served as the old histones according to the experimental design. Copurified native H3.1 and H4 histones were 3.0% and 3.4% K8-labeled, respectively (Fig. 1, C and D, and fig. S3). Thus, we conclude that the vast majority of H3.1-H4 tetramers follow the nonsplitting model. In contrast, copurified H2A and H2B were close to 50% K8-labeled, which resembles the overall pattern in the bulk histone preparation (Fig. 1C and fig. S3), indicating the extensive exchange of H2A-H2B dimers among nucleosomes.

At 72 hours, Flag-H3.1 histones were 3.8% K8-labeled (fig. S3), indicating minor leaky expression. Nonetheless, their associated native H3.1 and H4 histones remained in similar K8-labeling ranges (6.3% for H3.1 and 5.9% for H4), whereas copurified H2A and H2B histones were close to their bulk counterparts (fig. S3). Taken together, our data clearly demonstrate old Flag-H3.1 histones stay with old H3.1 and H4 histones at the mononucleosome level.

In a second set of experiments, we generated newly synthesized Flag-H3.1 histones by altering the timing of induction (fig. S4). After one

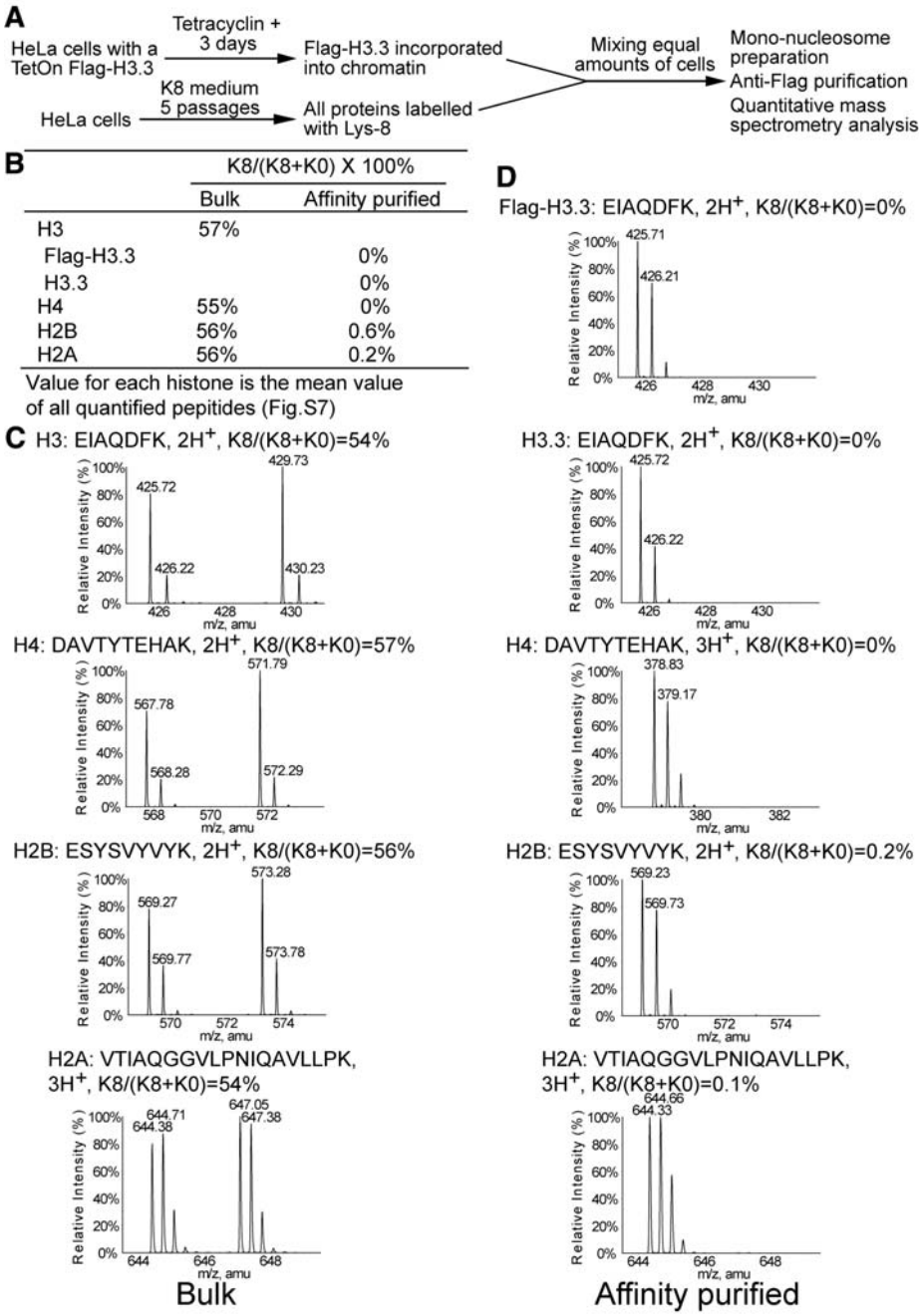

Fig. 3. H3.3-H4 tetramer splitting events occurred in vivo. (**A**) Experimental schemes. (**B**) Summary of K8-labeling status of bulk and affinity-purified histones. (**C** and **D**) Representative mass spectra for peptides derived from bulk core histones and affinity-purified core histones.

round of DNA synthesis, mononucleosomes were affinity-purified and subjected to quantitative mass spectrometry analysis. Flag-H3.1 histones were 93% K8-labeled and native H3.1 and H4 histones copurified with Flag-H3.1 were 90% and 92% K8-labeled, whereas bulk H3 and H4 histones were approximately 50% K8-labeled (fig. S4). In contrast, H2A and H2B histones copurified with newly synthesized Flag-H3.1 were approximately 50% K8-labeled, reflecting the level of labeling in bulk histones (fig. S4). These results indicate that newly synthesized Flag-H3.1 histones associate with newly synthesized native H3.1 and H4 histones, further supporting the H3.1-H4 tetramer nonsplitting model.

The experiments were then extended to the histone variant H3.3, which is known for marking active chromatin (*20*, *21*). We repeated the "on" to "off" experiments for H3.1 (Fig. 1) using the Flag-H3.3 stable cell line. At 36 hours, Flag-H3.3 histones were only 0.3% K8-labeled, indicating almost no leaky expression. However, copurified native H3.3 histones were 6.4% K8-labeled, reflecting a significant level of splitting events (Fig. 2, A and B, and fig. S5). Moreover, at 72 hours Flag-H3.3 was 2.8% K8-labeled, but copurified H3.3 histones were 23% K8-labeled (Fig. 2, A and C, fig. S5). Thus, about one fifth of the Flag-3.3/H4 tetramers had split within roughly two cell cycles. Given that two histone H4 molecules exist in each tetramer, one co-deposited with Flag-H3.3 and the other co-deposited with native H3.3, the density of H4 should lie between Flag-H3.3 and the native H3.3, which is indeed the case at both time points (Fig. 2). The above experiments were repeated in a second Flag-H3.3 stable cell clone that expresses at least fivefold less Flag-H3.3 (fig. S1A) without cell synchronization, and similar results were obtained (fig. S6).

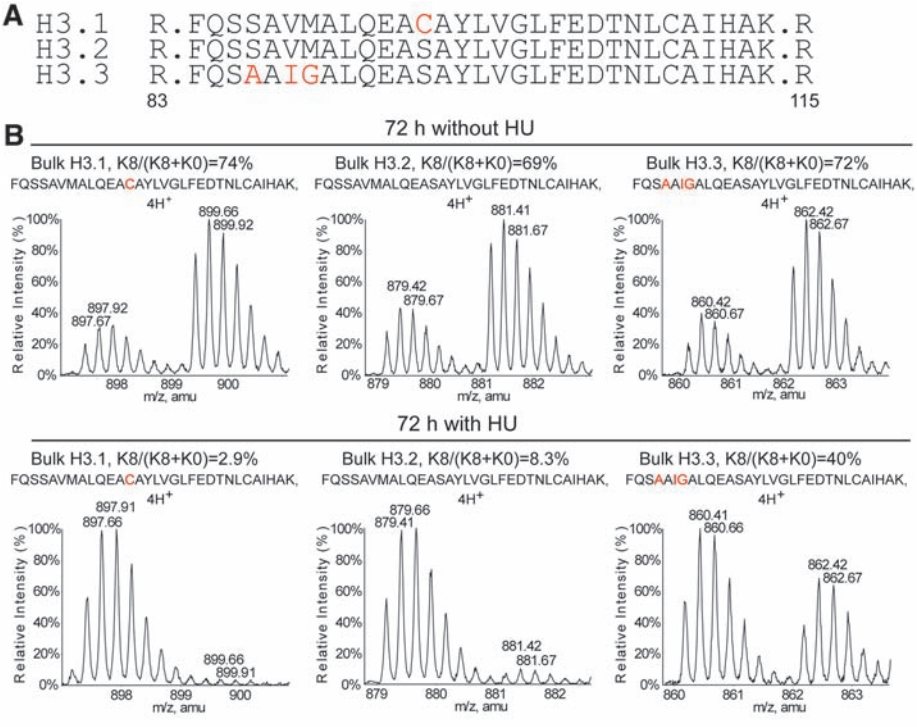

C

	K8/(K8+K0) X 100%			
	72 h without HU		72 h with HU	
	Bulk	Affinity purified	Bulk	Affinity purified
H3	77%		15%	
H3.1	74%		2.9%	
H3.2	69%		8.3%	
H3.3	72%	20%	40%	7.6%
Flag-H3.3		2.9%		1.0%
H4	76%	7.6%	13%	4.5%
H2B	78%	70%	25%	28%
H2A	82%	73%	32%	33%

Value for each histone is the mean value of all quantified peptides (Fig. S8)

Fig. 4. Inhibiting DNA replication greatly reduces the number of splitting events for H3.3-H4 tetramers. (**A**) H3 variants can be discriminated by a single tryptic peptide. Variant-specific amino acids are in red. The amino acid positions are indicated. (**B**) HU treatment strongly inhibits new H3.1 deposition while allowing replication-independent H3.3 deposition to occur. (**C**) Summary of K8-labeling status of bulk and affinity-purified histones from cells with or without HU treatment.

To further validate our conclusion, equal amounts of cells expressing Flag-H3.3 in regular medium were mixed with wild-type HeLa cells cultured in K8 medium. Mononucleosomes were then purified from the mixed cells and subjected to affinity purification with antibody to Flag and subsequent quantitative mass spectrometry analysis (Fig. 3A). In this control experiment, affinity-purified Flag-H3.3 histones showed no K8 labeling, and the copurified H3.3 and H4 histones also showed absolutely no K8 labeling. Even the relatively dynamic H2A and H2B histones were less than 1% K8-labeled (Fig. 3, B and D, and fig. S7), despite the existence of roughly 50% K8-labeled bulk histones in the starting material (Fig. 3, B and C, and fig. S7). These data clearly demonstrate the robustness of our assay system, thus ruling out the possibility that core histones might exchange among nucleosomes during the purification processes. Therefore, we conclude that the significant H3.3-H4 tetramer splitting events observed earlier (Fig. 2 and figs. S5 and S6) indeed occur in vivo.

Unlike canonical histones, which are deposited by the DNA replication–dependent pathway during S phase, H3.3 can also be deposited by a DNA replication–independent pathway (*16*, *20*). To test whether a replication-independent pathway is fully responsible for the splitting events, we performed the splitting assay using cells treated with hydroxyurea (HU) or aphidicolin, two reagents that arrest cells at S phase. These experiments allowed us to specifically study the replication-independent deposition pathway. The three H3 variants H3.1, H3.2, and H3.3 can be discriminated by a single peptide after trypsin digestion (Fig. 4A). We took advantage of this property, and successfully achieved individual quantification of H3.1, H3.2, and H3.3 in bulk histone preparations. Seventy-two hours of treatment with 2 mM HU almost fully inhibited the incorporation of new H3.1 (Fig. 4B), demonstrating strong inhibition of DNA replication. In contrast, newly deposited H3.3 accounted for ~40% of the total H3.3 (Fig. 4B), indicating that the replication-independent H3.3 deposition pathway remained effective. In addition, the splitting events in HU-treated cells were significantly reduced from the untreated control cells (7.6% versus 20%) (Fig. 4C and fig. S8). In a separate set of experiments, cells treated with 5 μg/ml aphidicolin displayed full inhibition of new H3.1 deposition while allowing incorporation of 53% new H3.3 in the same cells (fig. S9). Aphidicolin-treated cells also displayed a significantly lower level of splitting events (2.5%) in comparison with that of their parallel untreated control cells (11%) (fig. S9). These results collectively suggest that (i) the replication-independent H3.3 deposition pathway proceeds largely by cooperatively incorporating two new H3.3-H4 dimers and (ii) the majority of splitting events occurred during replication-dependent deposition, although detectable amounts of splitting events were observed during replication-independent deposition.

Our results support the idea that "silent" histone modifications within large heterochromatic regions are maintained by copying modifications from neighboring preexisting histones (*1*, *24*) without the need for H3-H4 splitting events. However, mechanisms underlying the mitotic inheritance of "active" modifications remain debatable. Our observation that significant amounts of H3.3-H4 tetramers split during replication-dependent nucleosome assembly brings up an intriguing question: Do these tetramer splitting events occur at specific regions of chromatin for specific functions, such as mitotic inheritance (*25*, *26*)? Although we observed significant splitting events only for H3.3–containing tetramers, it remains an open question whether such splitting events are variant-specific or rather chromatin region–specific. We did observe ~2% K8-labeling difference between Flag-H3.1 and copurified H3.1 in several experiments (Fig. 1 and figs. S3 and S4), which could be within our detection error but may also suggest splitting events for a small subset of H3.1–containing tetramers. One possible model is that the replication-dependent nucleosome assembly pathway differs at euchromatic and heterochromatic regions, resulting in specific splitting events, predominantly at euchromatic regions. This is particularly tempting because H3.3 is enriched in euchromatin (*20*, *21*, *27*), and H3.1 histones display a similar modification pattern in the vicinity of H3.3 histones (*22*). Detecting the "splitting hot spots" and unveiling their potential role in the mitotic inheritance of active modifications are interesting directions for future investigation.

References and Notes

1. C. D. Allis, T. Jenuwein, D. Reinberg, *Epigenetics* (Cold Spring Harbor Laboratory Press, New York, 2006).
2. T. Kouzarides, *Cell* **128**, 693 (2007).
3. R. Margueron, P. Trojer, D. Reinberg, *Curr. Opin. Genet. Dev.* **15**, 163 (2005).
4. R. Holliday, J. E. Pugh, *Science* **187**, 226 (1975).
5. T. H. Bestor, *EMBO J.* **11**, 2611 (1992).
6. R. L. Seale, *Cell* **9**, 423 (1976).
7. I. M. Leffak, R. Grainger, H. Weintraub, *Cell* **12**, 837 (1977).
8. G. Russev, R. Hancock, *Nucleic Acids Res.* **9**, 4129 (1981).
9. V. Jackson, R. Chalkley, *Cell* **23**, 121 (1981).
10. V. Jackson, R. Chalkley, *J. Biol. Chem.* **256**, 5095 (1981).
11. A. T. Annunziato, R. K. Schindler, M. G. Riggs, R. L. Seale, *J. Biol. Chem.* **257**, 8507 (1982).
12. C. P. Prior, C. R. Cantor, E. M. Johnson, V. G. Allfrey, *Cell* **20**, 597 (1980).
13. V. Jackson, *Biochemistry* **27**, 2109 (1988).
14. V. Jackson, *Biochemistry* **29**, 719 (1990).
15. K. Yamasu, T. Senshu, *J. Biochem.* **107**, 15 (1990).
16. H. Tagami, D. Ray-Gallet, G. Almouzni, Y. Nakatani, *Cell* **116**, 51 (2004).
17. C. M. English, N. K. Maluf, B. Tripet, M. E. Churchill, J. K. Tyler, *Biochemistry* **44**, 13673 (2005).
18. L. J. Benson *et al.*, *J. Biol. Chem.* **281**, 9287 (2006).
19. R. Natsume *et al.*, *Nature* **446**, 338 (2007).
20. K. Ahmad, S. Henikoff, *Mol. Cell* **9**, 1191 (2002).
21. Y. Mito, J. G. Henikoff, S. Henikoff, *Nat. Genet.* **37**, 1090 (2005).
22. A. Loyola, T. Bonaldi, D. Roche, A. Imhof, G. Almouzni, *Mol. Cell* **24**, 309 (2006).
23. J. J. Pesavento, H. Yang, N. L. Kelleher, C. A. Mizzen, *Mol. Cell. Biol.* **28**, 468 (2008).
24. J. Nakayama, J. C. Rice, B. D. Strahl, C. D. Allis, S. I. Grewal, *Science* **292**, 110 (2001).
25. Y. Nakatani, D. Ray-Gallet, J. P. Quivy, H. Tagami, G. Almouzni, *Cold Spring Harb. Symp. Quant. Biol.* **69**, 273 (2004).
26. A. V. Probst, E. Dunleavy, G. Almouzni, *Nat. Rev. Mol. Cell Biol.* **10**, 192 (2009).
27. S. Henikoff, J. G. Henikoff, A. Sakai, G. B. Loeb, K. Ahmad, *Genome Res.* **19**, 460 (2009).

28. We thank X. Wang from the Howard Hughes Medical Institute/University of Texas Southwestern Medical Center for critical comments on the manuscript. We thank N. Yang and J. Ni for color illustration. We thank P. Mortensen from the University of Southern Denmark for developing and supporting the MSQuant software. This work was supported by the Chinese Ministry of Science and Technology 863 projects 2007AA02Z1A6 (to B. Z.) and 2007AA02Z1A3 (to S.C.).

Supporting Online Material

www.sciencemag.org/cgi/content/full/328/5974/94/DC1
Materials and Methods
Figs. S1 to S9

13 July 2009; accepted 27 January 2010
10.1126/science.1178994

Dynamic Regulation of Archaeal Proteasome Gate Opening As Studied by TROSY NMR

Tomasz L. Religa,[1] Remco Sprangers,[2] Lewis E. Kay[1]*

The proteasome catalyzes the majority of protein degradation in the cell and plays an integral role in cellular homeostasis. Control over proteolysis by the 20*S* core-particle (CP) proteasome is achieved by gated access of substrate; thus, an understanding of the molecular mechanism by which these gates regulate substrate entry is critical. We used methyl–transverse relaxation optimized nuclear magnetic resonance spectroscopy to show that the amino-terminal residues that compose the gates of the α subunits of the *Thermoplasma acidophilum* proteasome are highly dynamic over a broad spectrum of time scales and that gating termini are in conformations that extend either well inside (closed gate) or outside (open gate) of the antechamber. Interconversion between these conformers on a time scale of seconds leads to a dynamic regulation of 20*S* CP proteolysis activity.

The 20*S* core-particle (CP) proteasome is a hollow, barrel-like structure that, through protein degradation, plays an important role in cellular homeostasis (*1*, *2*) and is a target for the design of inhibitors (*3*, *4*). The CP is composed of four homo-heptameric rings. In the case of the archaeal version, discussed here, each ring consists of seven identical monomers ($\alpha_7\beta_7\beta_7\alpha_7$), with the active sites sequestered inside the catalytic chamber formed by $\beta_7\beta_7$ (Fig. 1A) (*5*, *6*). Unfolded substrates enter the CP through the α annulus (Fig. 1, A and B), which is occluded by N termini of the α subunits (the gating residues). Although detailed x-ray structures (*6*–*8*) have established the overall architecture of the isolated archaeal CP, density has not been observed for the gating residues, and the molecular mechanism by which they control entry of substrates remains to be elucidated.

We have previously obtained high-quality ^{1}H-^{15}N transverse relaxation optimized spectroscopy (TROSY) (*9*) and ^{1}H-^{13}C methyl-TROSY (*10*) data sets for α_7 (*11*, *12*), a single-ring version of molecular weight = 180 kilodaltons. The N-terminal 35 residues could not be observed in amide spectra of α_7 (fig. S1), reflecting dynamics on the microsecond-millisecond time scale, which also severely attenuated peaks from isoleucine, leucine, and valine methyl groups in this region (fig. S2). We used a labeling scheme in which highly deuterated $^{13}CH_3$-methionine (Met) proteins were produced (*13*), so that Met methyl groups could be used as probes of structure and dynamics. The 20*S* CP α subunit contains only four natural Met residues, providing spectra of low complexity. To augment the two Met residues (M1 and M6) located in the gating termini, an additional Met residue (M-1) was introduced at the N-terminal end of the protein (Fig. 1C).

Methionine side-chains undergo large-amplitude, fast–time scale motions (*14*) that average out much of the conformational exchange broadening that affects other resonances, allowing high-quality Met methyl-TROSY spectra to be recorded. Figure 1D shows the ^{1}H-^{13}C correlation map of wild-type (WT) α_7. A total of 9 Met correlations were observed in the spectra, subsequently assigned via mutagenesis (fig. S3). Three peaks originate from each M-1 and M1 residue in WT α_7, corresponding to the major state ("A") and a pair of minor states ("B" and "C"). Similar multiple peaks were observed in spectra recorded on the intact WT $\alpha_7\beta_7\beta_7\alpha_7$ CP (Fig. 1D), establishing that they are not an artifact associated with the single-ring structure. Additionally, they do not emerge from the slightly longer-than-normal N terminus (Fig. 1C), as three peaks for M1 are also noted in spectra

[1]Departments of Molecular Genetics, Biochemistry, and Chemistry, University of Toronto, Toronto, Ontario M5S 1A8, Canada. [2]Max Planck Institute for Developmental Biology, Tübingen, Germany.

*To whom correspondence should be addressed. E-mail: kay@pound.med.utoronto.ca

Partitioning of Histone H3-H4 Tetramers During DNA Replication–Dependent Chromatin Assembly

Mo Xu, Chengzu Long, Xiuzhen Chen, Chang Huang, She Chen, and Bing Zhu

Science, **328** (5974), .
DOI: 10.1126/science.1178994

Histone Inheritance

Chromatin, the packaging material for eukaryotic genomes, is a potential repository for epigenetic information. The core structure of chromatin is the nucleosome, which consists of an octamer of histone proteins, two dimers each of histones H2A and H2B, and histones 3 and 4. Histones 3 and 4, in particular, carry a series of covalent modifications presumed to be passed on through cell division. Using mass spectrometry of tagged and isotope labeled histones, Xu *et al.* (p. 94; see the Perspective byRay-Gallet and Almouzni) followed the inheritance of the histones themselves through mitosis. The H2A-H2B dimers were inherited randomly through cell division, correlating with their lack of major covalent marks. In comparison, replication-deposited H3.1-H4 dimers did not separate through cell division, implying that H3 and H4 histone modifications might be maintained by copying from neighboring preexisting histones. Intriguingly, up to one-quarter of the nonreplication-deposited H3.3-H4 dimers, which mark active chromatin, did split during cell division.